# Interaction of Pt(II) and Au(III) with organic disulfide in hydrochloric aqueous solution

SCHOLARONE™
Manuscripts
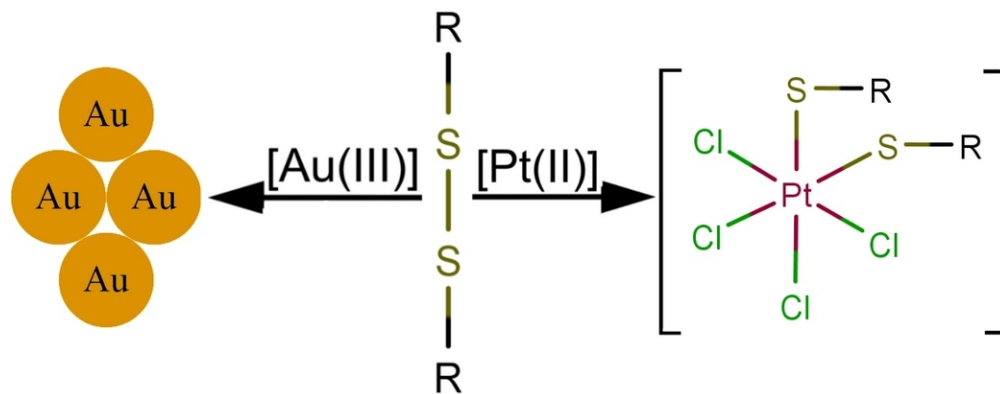
88x34mm (300 x 300 DPI)

# Interaction of Pt(II) and Au(III) with organic disulfide in hydrochloric aqueous solution

Alexander I. Petrov*[a], E-mail: sfupetrov@gmail.com
Galina V. Novikova[b], E-mail: gvnovikova1@gmail.com
Anastasia V. Demina[b], E-mail: ad329993@gmail.com
Timur Y. Ivanenko[b], E-mail: timivonk@gmail.com
Elizaveta S. Goleva[b], E-mail: Lizagoleva74@gmail.com

[a] Institute of Chemistry and Chemical Technology SB RAS, Federal Research Center "Krasnoyarsk Science Center SB RAS", Krasnoyarsk, Russian Federation
[b] Institute of Non-Ferrous Metals and Materials Science, Siberian Federal University, Krasnoyarsk, Russian Federation

*Corresponding author

The interaction of Pt(II) and Au(III) with disulfides (L-cystine, cystamine, DL-homocystine and 3,3'-dithiodipropionic acid) in hydrochloric acid aqueous solutions was studied. In the case of Pt(II), the oxidative addition reaction leads to the formation of the Pt(IV) thiol complex. In the case of Au(III) disulfide binding causes a reduction to Au(0) and oxidation of the disulfide to sulfonic acid. Cyclic voltammetry and different spectroscopic methods were used to study the process. The pattern of influence of the metallic properties for $d^8$ ions in the direction of the reaction was found.

*Keywords*: platinum(II); gold(III); organic disulfides; redox reactions; molecular spectroscopy

## Introduction

The interaction between platinum complexes and sulfur-containing biomolecules plays an important role in the metabolism of anticancer drugs [1]. Gold(III) and platinum(II) isostructural and isoelectronic complexes have been tested as potential candidates for cancer treatment. However, Au(III) is prone to the rapid oxidation of biomolecules, being consequently reduced to Au(I) or Au(0). Thus Au(III) is able to oxidize thiols and disulfides to the sulfonic acid. These reactions play an important role, causing the toxic side effects of gold-based drugs [2].

Apart from anticancer activities, platinum(II) complexes participate in oxidative addition and substitution reactions which lead to their applications as catalysts. The oxidative addition of the S–S bond to transition metal complexes is one route for activation of disulfides. The lower reactivity of platinum(IV) complexes with a coordination number of six lead to a decrease in their side effects. Thus, the synthesis of new platinum(IV) complexes with biochemical specifications can be very valuable. The interaction of platinum(II) with disulfides involves different mechanisms. They are complexation with the formation of polynuclear disulfide complexes [3, 4], disproportionation with the formation of thiol complexes of platinum(II) [5-7] and oxidative addition with the formation of thiol complexes of platinum(IV) [8-11].

Disulfide bonds play important roles in establishing and maintaining three-dimensional folding and structure of proteins. They can act as switches for protein function or as regulators for secreted proteins through bond cleavages. Disulfide redox systems control many important events

1

in cellular processes like regulating cell growth and cancer development. Cleavage of covalent disulfide bonds via reduction is a very important step in chemical reactions. In addition, organic disulfides might be used in the refinement of platinum metals from hydrochloric solutions [12].

The organic disulfides picked for this research are cystine, cystamine, homocystine and 3,3'-dithiodipropionic acid (Figure 1). The size of their carbon skeleton structure and their functional groups are different. Hence, the influence of the structure and redox properties of organic multifunctional disulfides on the state of a disulfide bond during interaction with d-metal ions and the effect of d-metal ion nature on the formation of specific reaction products becomes possible and worthwhile.

We have previously reported no disulfide bond cleavage takes place during the stepwise complex formation of L-cystine ($H_4CysS^{2+}$) [13, 14] and cystamine ($H_2Cyst^{2+}$) [15] with Pd(II) in hydrochloric acid solutions. On the other hand, we have reported irreversible disproportionation takes place during the interaction of homocystine ($H_4hCysS^{2+}$) and 3,3'-dithiodipropionic acid ($H_2DTDPA$) [16] with $Pd^{2+}$ yielding sulfinic ($RS(O_2H)M$) and thiol ($RSM$) complexes. This study extends the field of previous studies under similar conditions. The aim of the work is to gain more knowledge of the coordination chemistry of disulfides.

{Figure 1}

**Experimental Section**

*Materials*

All chemicals used were of analytical grade: $K_2PtCl_4$, $HAuCl_4 \cdot 4H_2O$, $C_7H_{14}N_2S_2O_4$ (dl-homocystine, $H_2hCysS$, 99%, Aldrich), $C_6H_{10}S_2O_4$ (3,3'-dithiodipropionic acid, $H_2DTDPA$, $\geq$ 98.0%, Aldrich), $C_4H_{14}N_2S_2Cl_2$ (Cystamine dihydrochloride, 99%, $H_2Cyst$, Aldrich), $C_6H_{12}N_2S_2O_4$ (Cystine, $H_2CysS$, 99%, Aldrich), $C_2H_5OH$ (ethanol, 96.0%), $HClO_4$, HCl, $Na_2CO_3$ and NaCl. Concentrations of HCl and $HClO_4$ have been determined titrimetrically with a standardized $Na_2CO_3$ solution. Stock solutions of $K_2PtCl_4$, dl-homocystine, and NaCl were prepared by dissolution of their accurate weights in distilled water. Stock solutions of $K_2PtCl_4$, $HAuCl_4$, $H_2hCysS$, $H_2HCyst$, and $H_2DTDPA$ also contained 0.5 M HCl. The $NaClO_4$ solution was prepared by neutralization of $Na_2CO_3$ with perchloric acid. The concentration of sodium perchlorate was determined gravimetrically in the form of $Na_2SO_4$. Since 3,3'-dithiodipropionic acid is not soluble in water, the accurate ligand weight was dissolved beforehand in the minimal volume of ethanol with a consequent adding of hydrochloric acid and distilled water for the necessary concentration and acidity.

*Equipment*

The UV-Vis electronic absorption spectra (EAS) were recorded with an Evolution 300 scanning spectrophotometer (ThermoScientific, England) using 1 cm quartz cells. Cell thermostating ($\pm$ 0.1 K) was performed with a Haake K15 thermostat connected to Haake DC10 controller. The absorbance was recorded within 220 - 450 nm.

The Hi-Res $^{13}$C-NMR spectra of aqueous and $d_6$-DMSO solutions were recorded with a Bruker Avance III spectrometer (600 MHz $^1$H-resonance gradient coil). The $D_2O/H_2O$ mixture served as an external standard. NMR spectra were acquired employing a gradient-based water suppression pulse sequence. The Fourier spectrum was obtained by transformation of 32K points and consequent convolution with exponential function with 0.8 Hz broadening. The NMR spectra

2

of all samples were complexified by radiation damping effect providing some lowering of NMR spectra quality. The $^{13}$C-NMR spectra were measured in conventional pi/2-excitation decay experiment with pulsed proton decoupling.

The cyclic voltammograms and polarograms were recorded on an IPC-Pro M potentiostat with computer software using a three-electrode system. The working electrode was a glassy carbon (GC) electrode of 5 mm diameter and graphite (G) electrode of 6 mm diameter. The auxiliary electrode was a platinum wire placed in a glass tube with a porous filter. The reference electrode was a saturated calomel electrode connected to the cell by an electrolytic bridge filled with background electrolyte through a Lungin's capillary. The disturbing influence of oxygen was eliminated by bubbling purified argon through the sample solution for 15–20 minutes. The number of electrons participating in each redox stage was determined by comparing the wave heights of the studied compounds with the two-electron wave height of a well-studied complex $K_2PtCl_4$. Measuring rate varied between 0.01 - 0.50 in / c.

The ICP-AES was performed with an iCAP 6500 spectrometer (ThermoScientifc, UK). Thermal gravimetric analysis (TGA) was performed by simultaneously using SDT-Q600 TA Instruments thermal analyzer coupled with FTIR spectrophotometer in the air atmosphere within 20–800 $^0$C at the scan rate of 10 K min$^{-1}$. From TG and DTG curves, some of the solid intermediate decomposition products were determined and were confirmed by the IR spectra.

The FTIR spectrum was obtained from a KBr pellet within 4000–400 cm1 with a Nicolet 6700 spectrometer. The Raman spectra were recorded with a Nicolet Almega XR Raman spectrometer at 785 nm excitation wavelength and 4 cm$^{-1}$ resolution.

The X-ray photoelectron spectra (XPS) were acquired using a SPECS spectrometer equipped with a PHOIBOS 150 MCD-9 analyzer (SPECS, Berlin, Germany) at an electron take-off angle of 90° employing monochromatic Mg Kα radiation (1253.6 eV) of an X-ray tube operating at 180 W. The Pt 4f7/2 and 4f5/2 doublets were fitted, after the subtraction of the Shirley-type background, with the coupled peaks with the Gaussian–Lorentzian peak profiles using the CasaXPS software package.

ESI-MS spectra were recorded on an LCMS-2010 LC/MS instrument equipped with a single quadrupole mass detector. The instrument was used as simple ESI-MS equipment, *i.e.*, the column was by-passed. The complex was dissolved in DMSO and further diluted with $CH_3OH$ (1:30). The sample was introduced into the ESI probe by manual injection with the use of a Hamilton Microliter syringe. Spectra were taken in negative mode. Optimal MS conditions were established by a series of preliminary experiments and the best operational parameters were: capillary voltage 4.5 kV, cone voltage 40 V, the flow of desolvation gas was 240 l/h, source temperature 125 °C, desolvation temperature 200 °C and range *m/z* 100-2500.

The samples for UV-Vis, Raman, NMR, and EXAFS spectroscopies were prepared according to Table 1.

{Table 1}

*Equilibrium studies*

The stoichiometry of complex species was determined by molar ratio, isomolar series, and Job's methods. The concentration of hydrochloric acid always exceeded 0.1 M in order to ensure the dominance of single chemical forms of both metal and ligand. Also, the disulfides are well

3

soluble and stable in the conditions specified, that allows performing investigations of $H_4CysS^{2+}$, $H_2Cyst^{2+}$, $H_4hCysS^{2+}$, and $H_2DTDPA$ interactions with $[PtCl_4]^{2-}$ and $[AuCl_4]^-$.

Hydrochloric acid was taken in excess to prevent $[PtCl_4]^{2-}$ hydrolysis. Each set of process solutions has included a solution of ligand ($C_L$), a series of solutions containing $K_2PtCl_4$ or $HAuCl_4$ ($C_M$) and a series of solutions containing both metal and ligand ($C_M + C_L$). Stability constants of complex species have been determined using the molar ratio method's data. The required acidity ($C_{H^+} = 0.1-1.0$ M) was provided with HCl and $HClO_4$, and ionic strength (I = 0.1-1.0) was maintained with NaCl and $NaClO_4$. The series of reactant solutions have been prepared from previously thermostatted ($\pm 0.1$ K) stock reagent solutions and was kept in darkness within a week ($\pm 0.1$ K). The absorbance was measured within 220–450 nm.

Determination of true chemical equilibrium was vindicated by invariance of EAS of work solutions in time (2-3 days) and reversibility of changes in absorbance (A) under heating or cooling a system. The absorbance was recovered to initial values in all spectral range under recovering of the temperature to initial 298 K.

Mathematical processing of UV-Vis EAS was carried out with Scilab 5.5.2 software. The statistical treatment was performed in the 95% confidence limit. The number of absorbing species N contributing to the absorbance matrix was estimated with the factor indication function (IND) [17]. Calculations of conditional stability (K') were performed by the non-linear LSR analysis using Absorbance matrix as raw data [18]. The optimal values for $K'_n$ and $\varepsilon^\lambda_n$ were found from the condition of least squares:

$$f(\mathbf{C_M}, \mathbf{C_L}, \mathbf{K'}, \boldsymbol{\varepsilon}) = \sum_{i=1}^{n} (A_i^\lambda - A_i^{calc})^2 \xrightarrow[\mathbf{K}, \boldsymbol{\varepsilon}]{} \min, (1)$$

where

$$A_{calc}^\lambda = \sum_{i=1}^{n+2} \varepsilon_i [S_i] = \varepsilon_L[L] + \varepsilon_M[M] + \sum_{i=1}^{n} [ML_i]\varepsilon_i, \quad (2)$$

Every equilibrium concentration was obtained by solving systems of mass balance equations and law of mass action.

*Synthesis of the complex [Pt(SCH2CH2CO2H)2Cl2]*

A solution of 0.104 g (0.25 mmol) of $K_2[PtCl_4]$ in 5 mL 0.1 M HCl was mixed with the suspension of 0.052 g (0.25 mmol) of 3,3'-dithiodipropionic acid in 5 mL 0.1 M HCl. A yellow-brown precipitate was formed at room temperature in several weeks. The solid complex was filtered and washed and dried in air to a constant weight. Yield 0.05 g (45%). Found, %: Pt 41,0; S 14,0. Calculated, %: Pt 40,96; S 13,47.

*Computational details*

Calculations were carried out using the GAMESS US program package [19]. Geometry optimization was performed by density functional theory (DFT) with the hybrid functional PBE0 [20] under Grimme's empirical correction [21] with no symmetry constraints. The def2-SVP basis set [22] including ECP pseudo-potential for Pt was applied to every atom in the complex during every computational procedure.

4

### Results and discussion

Process of complex formation causes changes of electronic absorption spectra (EAS): $\Delta A^\lambda = A^\lambda_{complex} - A^\lambda_{MCl4} - A^\lambda_L$ ($A^\lambda$ – absorbance at given wavelength, L = disulfide). $\Delta A$ depends on the concentration of the complex formed and serves as raw data for quantitative calculation of complex formation. Numbers of absorbing species N contributing to the absorbance matrix was estimated in the 310 – 450 nm range, where the absorbance of ligands is negligible. N is equal to 3 at $C_M > C_L$, thus $[PtCl_4]^{2-}$ and two complexes are the only absorbing species in the solution. The complex formation processes reached "true" equilibrium within 10 days; this was evidenced by the constancy of EAS by that time. The reversibility of spectroscopic changes after both heating and cooling of the system also confirmed "true" equilibrium. Common EAS of Pt(II) - $H_4CysS^{2+}$ and Au(III) - $H_2DTDPA$ hydrochloric solutions are shown in Figure 2. It can be noted that the spectral changes have one maximum, which did not depend on the concentration of metal and on the character of the disulfide. For Pt(II) - disulfide systems, the band wavelength lied within 253-257 nm. For Au(III) - disulfide systems, the absorption maximum of $AuCl_4^-$ (314 nm) disappears, which means the formation of Au(I).

{Figure 2}

The stoichiometry of interactions was determined by a molar ratio, isomolar series and Job's methods (Figure 3 (A-C)). One might conclude the coordination model was invariant in the studied conditions. The strong binuclear complex and a monocomplex was found for Pt(II) - disulfide systems, which was consistent with the calculated number of absorbing species in the solution. Calculated spectral profile for the Pt(IV) thiol complex presented in Figure 3D.

The values of the calculated "condition" equilibrium constants ($K_1'$) are given in Table 2. Conditional stability constant ($K_1'$) does not depend on the concentration of chloride ions and the acidity of the solution. This is contrary to stepwise complexing and may be explained by the formation of a thiol complex Pt(IV):
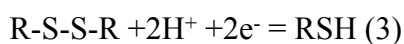
$$R\text{-}S\text{-}S\text{-}R + [PtCl_4]^{2-} = [Pt^{IV}Cl_4(S\text{-}R)_2]\ (1)$$
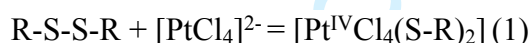
{Figure 3}

The formation of the S,S'-binuclear complex is competitive process:

$$R\text{-}S\text{-}S\text{-}R + 2[PtCl_4]^{2-} = [Pt_2Cl_6(R\text{-}S\text{-}S\text{-}R)]^{2-} + 2Cl^-\ (2)$$
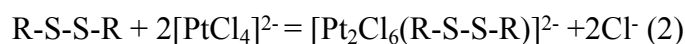
The formation of a Pt–S bond is observed for both cases and is common for platinum chemistry. Similar interactions (2) play an important role in the two-electron thiol-disulfide equilibrium:

$$R\text{-}S\text{-}S\text{-}R + 2H^+ + 2e^- = RSH\ (3)$$

{Table 2}

5

Presence of Pt(IV) was confirmed by electrochemical studies of solutions of the complexes after reaching equilibrium. For this purpose, voltammograms of the blank background electrolyte, of the background electrolyte with the addition of ligand and of the background electrolyte containing both metal ion and ligand were recorded using the graphite (G) electrode. The redox potentials values on a graphite electrode are given in Table 3. No oxidation waves on voltammograms were recorded (Figure 4A), and an irreversible two-electron reduction wave was recorded at $\approx$ -0.95 V vs. SCE due to the transition of $Pt^{4+}$ to $Pt^{2+}$. The reduction of cystine in hydrochloric acid solutions has been studied previously [23]. Irreversible diffusion-controlled reduction of L-cystine to cysteine occurs at -0.45 V vs. SCE. Other disulfides have similar potential values $\approx$ -0.6 V (Table 3). Therefore, a peak of -0.95 V refers to the recovery of the complex. This experiment confirmed the formation of the Pt(IV) thiol complex in hydrochloric acid aqueous solutions.

{Table 3}

{Figure 4}

Concentrated solutions are formed in the Pt(II) - $H_4hCysS^{2+}$ system without precipitation. NMR spectra were recorded for an equilibrium mixture. Beforehand, we reported that $^{13}C$-NMR spectroscopy provided essential data on the state of a disulfide bond [15]. Analysis of the NMR data (Table 4) for the system Pt(II) – $H_4hCysS^{2+}$ confirmed the formation of the Pt(IV) thiol complex in solution. Changes in the $C_\alpha$ and $C_\beta$ (numeration goes from sulfur) environments can be easily observed comparing $^{13}C$ NMR spectra for free $H_4hCysS^{2+}$ and a complex. They confirm the formation of the Pt - S bond. The chemical shift for $C_\alpha$ is decreased that is consistent with the formation of the platinum thiol complex. There is no new chemical shift at 57 ppm in the $^{13}C$ NMR spectrum, which refers to the products of disproportionation or oxidation. There is no difference in the $^{13}C$ NMR spectra between the chemical shift of carbon associated with the -$SO_2H$ or –$SO_3H$ group. For a disproportionation reaction and the oxidation appears characteristic chemical shift at 57 ppm in $^{13}C$ NMR.

{Table 4}

The thiol complex of Pt(IV) was isolated in the interaction of 3,3'-dithiodipropionic acid with $PtCl_4^{2-}$. The $[Pt(SCH_2CH_2CO_2H)_2Cl_2]$ complex was found to be X-ray amorphous according to XRD analysis. An attempt to grow a single crystal has also failed. The complex is insoluble in dichloromethane, water, chloroform, and alcohols, but is soluble in DMSO, and DMF. Complexes with cystine, cystamine, and homocystine in the studied conditions could not be isolated.

The IR spectrum for the $[Pt(SCH_2CH_2CO_2H)_2Cl_2]$ complex (Figure 5A) exhibits a strong absorption band at 1705 $cm^{-1}$ which was assigned to the protonated carboxylic group. In addition, the broad band with a maximum at 3447 $cm^{-1}$ in the spectrum of the complex was assigned to the stretching mode of the O-H group from the protonated COOH group [24].

The $^{13}C$ NMR spectrum (Table 4) of the complex in $d_6$-DMSO showed signals at $\delta$ 28.9 ($C_\alpha$), 171.8 (COOH). Additional signal overlaps with the signal from the solvent. Similar chemical shifts were obtained for the Pd(II) - $H_2DTDPA$ system in which the Pd(II) thiol complex is formed [15]. Chemical shifts for free $H_2DTDPA$ are found at 33 ($C_\alpha$), 34 ($C_\beta$), 175 (COOH) ppm. The $^{13}C$

6

signals shift downfield from free ligand's 33 ppm to 28.9 ppm and shift upfield from 175 ppm to 171.8 ppm. Its confirm the formation of S,O-chelate thiol platinum complexes.

The complex was characterized using ESI mass spectrometry (Figure S1); the complex was dissolved in a small quantity of a solvent (DMSO) in which it is soluble, and then diluted with methanol. In negative-ion mode, the expected ion $\{[Pt_2(\mu\text{-}SCH_2CH_2CO_2H)_2Cl_2]\cdot 2DMSO\text{-}H\}^-$ ($m/z$ 848.899, calculated $m/z$ 848.888) was observed in the DMSO-methanol solution. Molecular ion of $[Pt(SCH_2CH_2CO_2H)_2Cl_2]$ was not detected. However, the spectra were relatively complex, and a number of ions were unable to be assigned. The formation of $[Pt_2(\mu\text{-}SCH_2CH_2CO_2H)_2Cl_2]$ as the main product is not consistent with all other data.

The TGA study (Figure 5B) of the complex showed that it was stable up to 180°C. The decomposition of the complex began at 200°C and terminated at 400°C. The decomposition of the complex in the temperature range 400–800°C led to the formation of the $PtO_2$ (weight loss: exp. 51.1%, calc. 52.3%). The TG–FTIR analysis (Figure S2) of the gaseous species produced by the thermal degradation in the air using standard IR spectra made evident the following: 200 – 250 °C: HCl, $SO_2$, COS, acrylic acid; >400 °C: $CO_2$, $SO_2$. The decomposition of the complex in the temperature range 200–250°C led to the formation of the $[Pt_2(\mu\text{-}SCH_2CH_2CO_2H)_2Cl_2]$ (weight loss: exp. 31.9%, calc. 29.5%). Its formation is proposed based on the results ESI-MS. Scheme 1 shows thermal decomposition products.

{Scheme 1}

Cyclic voltammogram of $[Pt(SCH_2CH_2CO_2H)_2Cl_2]$ in DMSO are shown in Figure 4B. The peak at -0.85 V vs. SCE corresponds to the irreversible two electron reduction of complex, which agrees with the CV data for hydrochloric acid solution (Figure 4A). We also carried out X-ray photoelectron spectroscopy to confirm the oxidation state of platinum. XPS spectra have two peaks, which deconvoluted into four components with the binding energies of 72.2, 74.0 eV, 75.5 eV, and 77.5 eV. Typical signals at 75.5 and 77.5 eV were assigned to the 4f7/2 and 4f5/2 peaks of Pt(IV) according to the signals of standard $K_2PtCl_6$, indicating the presence of +4 oxidation state of Pt ion [25]. Another pair of peaks at ca. 72.2 eV (4f7/2) and 75.5 eV (4f5/2) belonged to Pt(II) species according to the signals of standard $K_2PtCl_4$, which may be a result of the decomposition of $[Pt(SCH_2CH_2CO_2H)_2Cl_2]$ to $[Pt_2(\mu\text{-}SCH_2CH_2CO_2H)_2Cl_2]$.

{Figure 5}

The isolated complex confirmed the formation of the Pt(IV) thiol complex and the course of the oxidative addition reaction. For example, the complex $[Pt(SCH_2CH_2CO_2H)_2]$ is a possibility of formation S,O-chelates platinum complexes with coordination through the oxygen atom of the protonated carboxylic groups [26]. A view of the DFT-optimized structures for S,O-chelate $[Pt(SCH_2CH_2CO_2H)_2Cl_2]$ complex is shown in Figure 6. As can be seen from the optimized geometries the complex may exist in four isomers. The most favorable form is the **D** isomer (cis, cis) and axial bonds are longer than equatorial. The length of the bonds d(Pd-S): DFT 2.294 Å and 2.345 Å; exp. 2.292 Å and d(Pd-O): DFT 2.116 Å and 2.209 Å; exp. 2.143 Å are consistent with experimental data for a similar complex - (2,2'-Bipyridine-k²N,N')-dimethyl(3-sulfidopropionato-k²S,O)-platinum(IV) [27].

{Figure 6}

7

In the case of Au(III) spectral changes suggested an irreversible interaction with disulfide took place (Figure 7A). The ratio of M:L = 3.3:1, and the elemental (metallic) gold was yielded upon reaction confirming a previously reported reaction [2]. For diselenides, a similar reaction (4) takes place [28]:

$$10[AuCl_4]^- + 3R\text{-}S\text{-}S\text{-}R + 18H_2O = 6R\text{-}SO_3H + 10Au^0 + 40Cl^- + 30H^+ \quad (4)$$

{Figure 7}

Hydrogen peroxide oxidizes disulfides to sulfonic acid. Therefore, the Raman spectra were recorded for Au(III) - disulfide ($C_M : C_L = 4:1$) and disulfide - $H_2O_2$ ($C_{H2O2} : C_L = 10:1$) systems in hydrochloric acid to compare products. The Raman spectra exhibited almost no difference, except for the band at 872 cm$^{-1}$, which referred to $\nu_s(O\text{-}O)$, and the band at 345 cm$^{-1}$, which refers to $\nu_s(Au\text{-}Cl)$. This band confirmed the formation of the same products. In the Raman spectrum (Figure 7B), a strong band was observed at 1042 cm$^{-1}$ referring to the oscillation $\nu_s(S=O)$ and confirming the formation of -SO$_3$H. In the Raman spectrum, a band of weak intensity was observed within 1000-1100 cm$^{-1}$ during the formation of R-SO$_2$H. It is in the area 1000 – 1100 cm$^{-1}$ [24]. The investigated samples of platinum complexes exhibited luminescence, hence we wouldn't be able to scan Raman spectra. Electrochemical research of Au(III) - disulfide systems did not provide additional information about the reaction products. We will present the features of interaction kinetics in the selected systems in the following articles.

The standard electrode potentials for the thiol-disulfide pairs (-0.25 V) [29], the disulfide bond length d(S-S) = 2.04 Å and the torsion angle <(C-S-S-C) = 82° were close for the selected disulfides [30]. However, the reaction products are different. Standard redox potentials: [PdCl$_4$]$^{2-}$/Pd$^0$ = 0.623 V, [PdCl$_6$]$^{2-}$/[PdCl$_4$]$^{2-}$ = 1.288 V, [PtCl$_6$]$^{2-}$/[PtCl$_4$]$^{2-}$ = 0.72 V, [PtCl$_4$]$^{2-}$/Pt = 0.73 V, [AuCl$_4$]$^-$/[AuCl$_2$]$^-$ = 0.926 V and [AuCl$_2$]/Au = 1.15 V. Thus, there is a dependence of the direction of the reaction on the character of the d$^8$ metal. We did not find the interaction of NiCl$_2$ in hydrochloric acid solutions with the selected disulfides. The structure of the disulfides studied has an effect on the reaction rate, not on the direction. This is shown in our work on the experimental and quantum chemical study of the interaction of Pd(II) with disulfides [31]. Based on the analysis of the products of the interaction of Ni(II), Pd(II), Pt(II) and Au(III) with disulfide in hydrochloric acid aqueous solutions, the square planar complexes with d$^8$ configuration react with disulfides:

1. Stepwise complexation or disproportionation reaction takes place for metal not prone to redox processes (for example, palladium(II)). The reaction of disproportionation proceeded through the formation of a binuclear S,S'-complex, which directs the reaction route to stepwise complexation (if this complex is not formed) or to hydrolysis.
2. The reaction of two-electron oxidative addition proceeds for an easily oxidizable metal (for example, platinum(II)). Also, the possibility of a reversible one-electron addition (for example, copper(I), cobalt(II)).
3. Disulfide oxidation to sulfonic acid and metal reduction proceeds for a metal exhibiting oxidative capacity (for example, gold(III)).

8

## Conclusion

The interaction of Pt(II) and Au(III) with disulfides (L-cystine, cystamine, DL-homocystine and 3,3'-dithiodipropionic acid) in hydrochloric acid aqueous solutions was studied by different spectroscopic methods and cyclic voltammetry. It was found that Pt(II) enters into the reactions of oxidative addition and stepwise complexation, while Au(III) oxidizes disulfides. The $[Pt(SCH_2CH_2CO_2H)_2]$ complex has been synthesized and characterized by $^{13}C$ NMR, IR, ESI-MS, TG-FTIR, and computational methods.

## Acknowledgments

## Supplementary material

Supplementary data associated with this article can be found in the online version: http://dx.doi.org/xxxx.

## References

[1] X. Wang, Z. Guo, *Anti-Cancer Agents in Medicinal Chemistry,* **7,** 19 (2007)

[2] C.F. Shaw, M.P. Cancro, P.L. Witkiewicz, J.E. Eldridge, *Inorg. Chem.*, **19,** 3198 (1980)

[3] B.Đ. Glišić, S. Rajković, Z.D. Stanić, M.I. Djuran, *Gold Bull.*, **44,** 91 (2011)

[4] T. Swain, M. Prakash, *Aust. J. Chem.*, **62**, 493 (2009).

[5] A.K. Fazlur-Rahman, J.G. Verkade, *Inorg. Chem.*, **31**, 2064 (1992)

[6] S. Fakih, V. Munk, M. Shipman, P. Murdoch, J. Parkinson, P. Sadler, *Eur. J. Inorg. Chem.*, 1206 (2003)

[7] H. Wei, X. Wang, Q. Liu, Y. Mei, Y. Lu, Z. Guo, *Inorg. Chem.,* **44**, 6077 (2005)

[8] M. Noori, B. Shafaatian, B. Notash, *Inorganica Chim. Acta.*, **485**, 1 (2019).

[9] H. F. Niroomand, M. Rashidi, S.M. Nabavizadeh, *J. Mol. Struct.*, **1125**, 20 (2016)

[10] K.J. Bonnington, M.C. Jennings, R.J. Puddephatt, *Organometallics*, **27**, 6521 (2008)

[11] M.S. McCready, R.J. Puddephatt, *Inorg. Chem. Commun.*, **14**, 210 (2011)

[12] V.N. Losev, E.V. Elsuf'ev, E.V. Buiko, A.K. Trofimtchuk, E.V. Andrianova. *Mendeleev Commun.*, **14**, 24 (2004).

[13] A.I. Petrov, N.N. Golovnev, A.A. Leshok, *J. Coord. Chem.,* **65**, 1339 (2012)

[14] A.I. Petrov, I.D. Dergachev, N.N. Golovnev, *J. Coord. Chem.,* **69**, 748 (2016)

[15] A.I. Petrov, I.D. Dergachev, N.N. Golovnev, A.A. Kondrasenko, S.B. Erenburg, S.V. Trubina, *J. Coord. Chem.,* **70**, 2280 (2017)

[16] A.I. Petrov, I.D. Dergachev, N.N. Golovnev, *Polyhedron,* **157**, 479 (2019)

[17] M. Meloun, J. Čapek, P. Mikšík, R.G. Brereton, *Analytica Chimica Acta*, **423**, 51 (2000)

[18]    D.J. Leggett, *Computational methods for the determination of formation constants*, Plenum Press, NY (1985)

[19]    M. W. Schmidt, K. K. Baldridge, J. A. Boatz, S. T. Elbert, M. S. Gordon, J.H. Jensen, S. Koseki, N. Matsunaga, K. A. Nguyen, S.Su, T. L. Windus, M. Dupuis, J. A. Montgomery, *J. Comput. Chem.,* **14**, 1347 (1993)

[20]    C. Adamo, V. Barone, *J. Chem. Phys.*, **110**, 6158 (1999).

[21]    S. Grimme, J. Antony, S. Ehrlich, H. Krieg, *J. Chem. Phys.,* **132**, 154104 (2010)

[22]    F. Weigend, R. Ahlrichs, *Phys. Chem. Chem. Phys.*, **7**, 3297 (2005)

[23]    T.R. Ralph, M.L. Hitchman, J.P. Millington, F.C. Walsh, J. Electroanal. Chem., **587**, 31 (2006)

[24]    K. Nakamoto, *Infrared and Raman spectra of inorganic and coordination compounds*, Wiley, New York (2009)

[25]    Y. Ning, Y. Yu, Y.-W. Liu, J. Zhang, H.-L. Sun, J.-L. Zhang, *Porphyrins Phthalocyanines,* **20,** 785 (2016)

[26]    M. Chandrasekharan, M. R. Udupa, G. Aravamudan, *J. Inorg. Nucl. Chem.*, **36**, 1153 (1974)

[27]    M.S. McCready, R. J. Puddephatt, *Acta Cryst.,* E67, m604 (2011)

[28]    A.A. Isab, W. Ashraf, *Inorg. Chem. Commun.,* **8**, 358 (2005)

[29]    K.K. Millis, K.H. Weaver, D.L. Rabenstein, *J. Org. Chem.,* **58**, 4144 (1993)

[30]    D. Carrillo, *Coord. Chem. Rev.,* **119**, 137 (1992)

[31]    A.I. Petrov, I.D. Dergachev, *J. Phys. Chem. A,* **123**, 4873 *(*2019)

**Table 1.** Sample preparations

| Method | Conditions |
|---|---|
| Raman, NMR | $C_{Pt} = 0.2$ M, $C_L = 0.1$ M, $C_{HCl} = 0.25$ M |
| | $C_{Au} = 0.4$ M, $C_L = 0.1$ M, $C_{HCl} = 0.25$ M |
| Uv-Vis: | |
| molar ratio | $C_M = 7.5 \cdot 10^{-5}$ M, $C_L = 2.5 \cdot 10^{-5}$ M $- 1.0 \cdot 10^{-3}$ M, $C_{HCl} = 0.1$-$0.5$M |
| isomolar series | $C_L = 3.0 \cdot 10^{-4}$ M, $C_M = 4.0 \cdot 10^{-5}$ M $- 1.0 \cdot 10^{-3}$ M, $C_{HCl} = 0.25$M |
| Job's method | $C_M + C_L = 5.0 \cdot 10^{-4}$ M, $C_{HCl} = 0.25$M |

11

1
2
3
4
5
6
7
8
9
10
11
12
13
14
15
16
17
18
19
20
21
22
23
24
25
26
27
28
29
30
31
32
33
34
35
36
37
38
39
40
41
42
43
44
45
46
47
48
49
50
51
52
53
54
55
56
57
58
59
60

**Table 2**. The values of the $\log K_1'$

| Condition | Ligand | | | |
|---|---|---|---|---|
| | $H_2DTDPA$ | $H_4hCysS^{2+}$ | $H_2Cyst^{2+}$ | $H_4CysS^{2+}$ |
| HCl (0.25 M) | $3.59 \pm 0.05$ | $3.70 \pm 0.05$ | $3.35 \pm 0.05$ | $3.95 \pm 0.05$ |
| HCl (0.25 M)I(1) | $3.18 \pm 0.04$ | $3.60 \pm 0.05$ | $3.84 \pm 0.05$ | $3.64 \pm 0.05$ |
| HCl (1 M) | $3.31 \pm 0.05$ | $3.40 \pm 0.05$ | $3.35 \pm 0.05$ | $3.15 \pm 0.04$ |

12

**Table 3.** Electrochemical characteristics of platinum complexes (G, V = 25 мВ/c, V vs SCE)

| Systems | $E_{1/2}$, B (n*) | |
|---|---|---|
| | Oxidation | Reduction |
| Pt(II) - $H_2Cyst^{2+}$ in $C_{HCl}$ = 0.25 M | — | -0.96 (2) |
| Pt(II) - $H_4CysS^{2+}$ in $C_{HCl}$ = 0.25 M | — | -0.93(2) |
| Pt(II) - $H_4hCysS^{2+}$ in $C_{HCl}$ = 0.25 M | — | -0.99 (2) |
| Pt(II) + $H_2DTDPA$ in $C_{HCl}$ = 0.25 M | — | -0.94(2) |
| $K_2PtCl_4$ in $C_{HCl}$ = 0.25 M | 0.98(2) | -0.57(2) |
| [Pt(SCH$_2$CH$_2$CO$_2$H)$_2$Cl$_2$] in DMSO | — | -0.85 (2) |
| $H_2Cyst^{2+}$ in $C_{HCl}$ = 0.25 M | — | -0.58 (2) |
| $H_4CysS^{2+}$ in $C_{HCl}$ = 0.25 M | — | -0.56 (2) |
| $H_4hCysS^{2+}$ in $C_{HCl}$ = 0.25 M | — | -0.60 (2) |
| $H_2DTDPA$ in $C_{HCl}$ = 0.25 M | — | -0.62 (2) |

*n – numbers of electrons involved in the electrode reaction

13

**Table 4**. Data of NMR spectroscopy

| $H_4hCysS^{2+}$ (aq) | | Pt(II) - $H_4hCysS^{2+}$ (aq) | | $H_2DTDPA$ (DMSO) | | $[Pt(SCH_2CH_2CO_2H)_2Cl_2]$ (DMSO) | |
|---|---|---|---|---|---|---|---|
| $^{13}C$ δ | Assign. | $^{13}C$ δ | Assign. | $^{13}C$ δ | Assign. | $^{13}C$ δ | Assign. |
| 29 | $C_α$ | 23 | $C_α$ | 33 | $C_α$ | 28.9 | $C_α$ |
| 32 | $C_β$ | 35 | $C_β$ | 34 | $C_β$ | 171.8 | COOH |
| 52 | $C_γ$ | 52 | $C_γ$ | 175 | COOH | | |
| 172 | COOH | 171 | COOH | | | | |

14

**Figure 1**. Structures of L-cystine (A), cystamine (B), D,L-homocystine (C), and 3,3'-dithiodipropionic acid (D)

**Figure 2**. EAS (A, C) and $\Delta A$-$\lambda$ (B) plots for the Pt (II) - $H_4CysS^{2+}$ (A, B) and Au (III) - $H_2DTDPA$ (C) in 0.25 M HCl

**Figure 3**. Molar ratio (A), isomolar series (B) and Job's (C) methods and spectral profile (D) for Pt(II) - disulfide systems (1 - $H_4CysS^{2+}$, 2 - $H_2Cyst^{2+}$, 3 - $H_4hCysS^{2+}$, 4 - $H_2DTDPA$) at 0.25 M HCl

**Figure 4**. Cyclic voltammograms of Pt(II) - $H_4CysS^{2+}$ system in aqueous hydrochloric solution (G, $d_э$ = 5 mm, 0.25 M HCl, C = 2.5 mM, V vs SCE, scan rate 25 mV s$^{-1}$ ) and [Pt(SCH$_2$CH$_2$CO$_2$H)$_2$Cl$_2$] complex in DMSO containing 0.1 M TBAHFP (C = 2 mM scan rate 100 mV/s); 1 – complex, 2 – background

**Figure 5**. IR spectra (A) and TGA/DSC curves (B) for [Pt(SCH$_2$CH$_2$CO$_2$H)$_2$Cl$_2$] complex

**Figure 6**. DFT optimized structures of the [Pt(SCH$_2$CH$_2$CO$_2$H)$_2$Cl$_2$] at PBE0-D3/Def2-SVP level

**Figure 7**. Molar ratio method (A) for systems Au(III) - disulfides (1 - $H_4CysS^{2+}$, 2 - $H_2DTDPA$, 3 - $H_2Cyst^{2+}$, 4 - $H_4hCysS^{2+}$) and Raman spectra (B) of Au(III) - $H_2DTDPA$ (1) and $H_2DTDPA$ - $H_2O_2$ (2) systems in 0.25 M HCl

Scheme 1. Proposed thermal fragmentation of [Pt(SCH$_2$CH$_2$CO$_2$H)$_2$Cl$_2$] complex

.

15

1
2
3
4
5
6
7
8
9
10
11
12
13
14
15
16
17
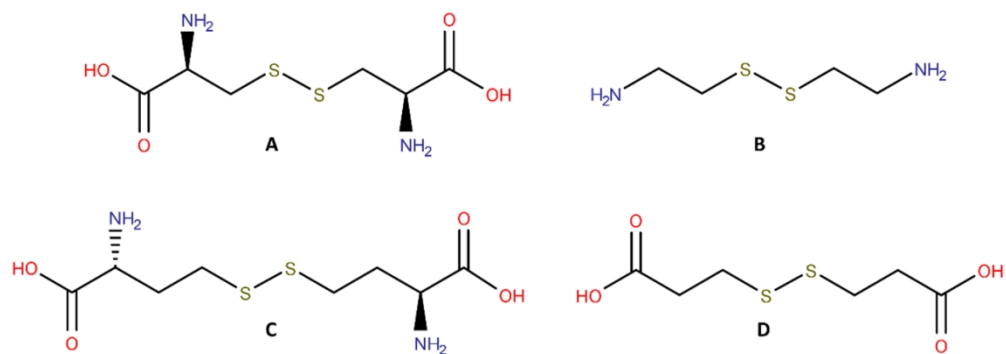


Figure 1. Structures of L-cystine (A), cystamine (B), D,L-homocystine (C), and 3,3'-dithiodipropionic acid (D)

349x122mm (96 x 96 DPI)

18
19
20
21
22
23
24
25
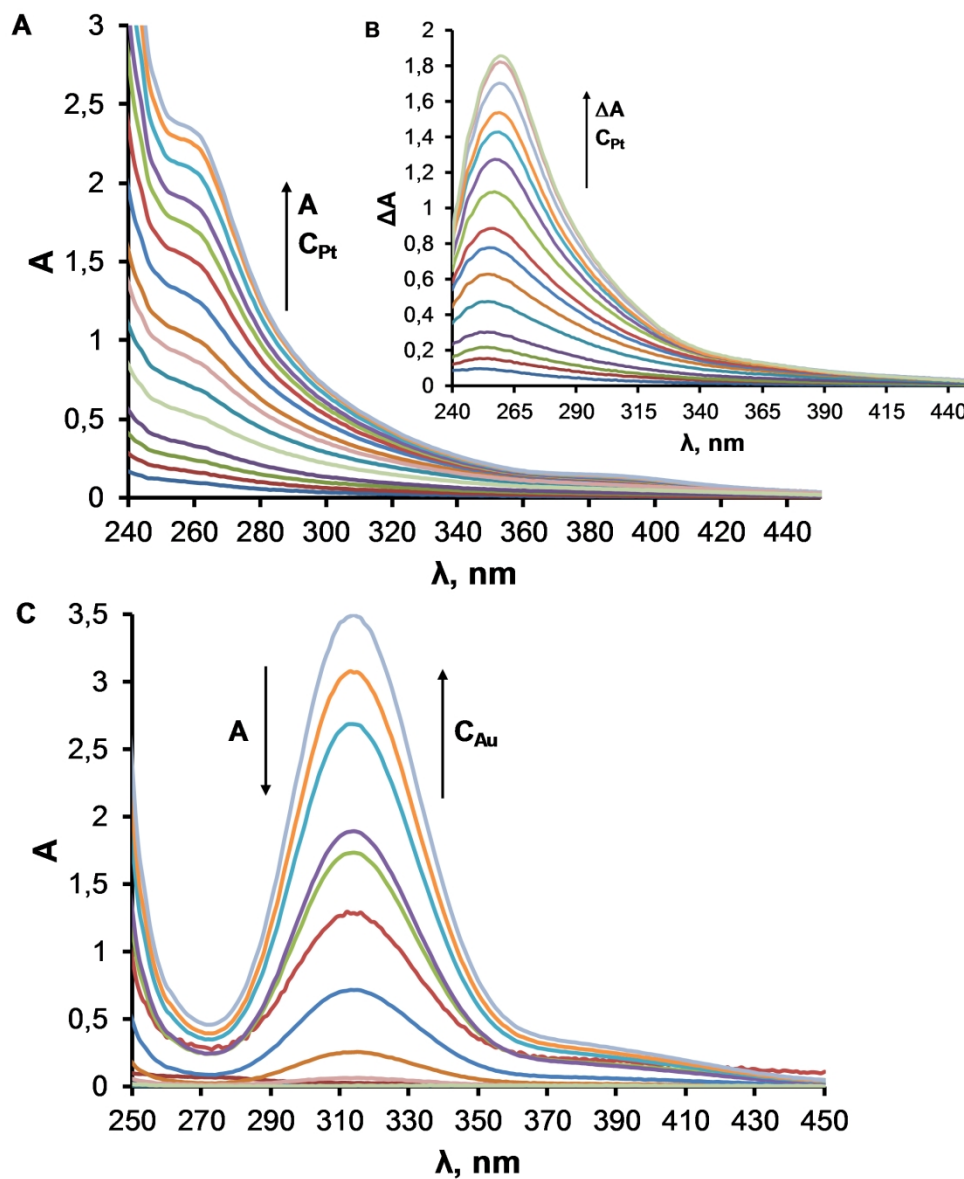26
27
28
29
30
31
32
33
34
35
36
37
38
39
40
41
42
43
44
45
46
47
48
49
50
51
52
53
54
55
56
57
58
59
60

Figure 2. EAS (A, C) and ΔA-λ (B) plots for the Pt (II) - H4CysS2+ (A, B) and Au (III) - H2DTDPA (C) in 0.25 M HCl

196x231mm (300 x 300 DPI)

1
2
3
4
5
6
7
8
9
10
11
12
13
14
15
16
17
18
19
20
21
22
23
24
25
26
27
28
29
30
31
32
33
34
35
36
37
38
39
40
41
42
43
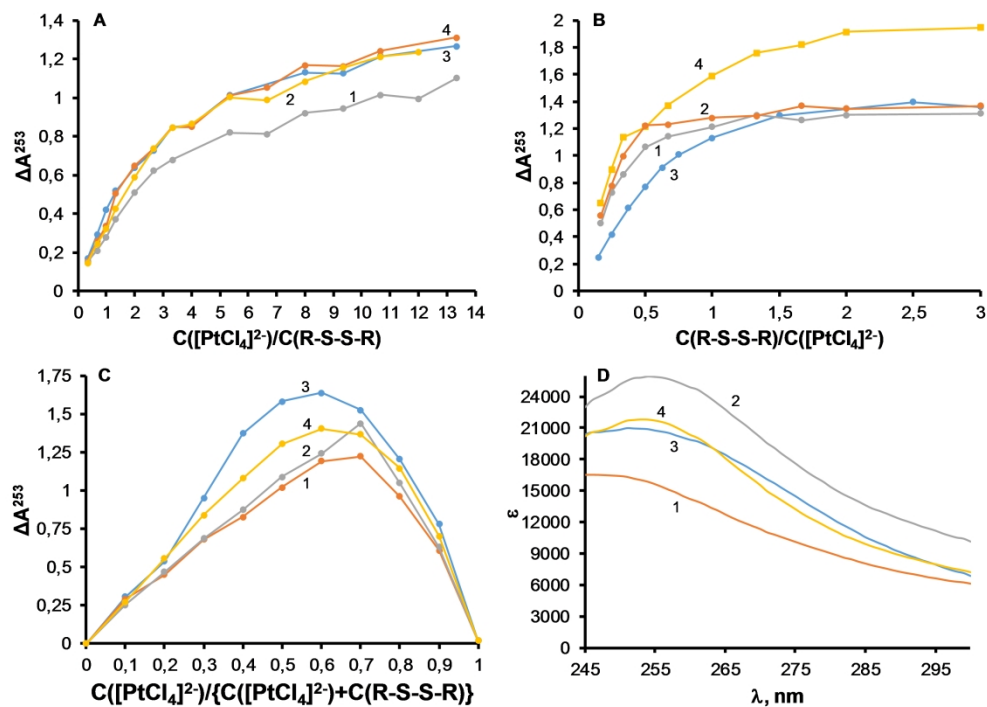44
45
46
47
48
49
50
51
52
53
54
55
56
57
58
59
60



Figure 3. Molar ratio (A), isomolar series (B) and Job's (C) methods and spectral profile (D) for Pt(II) - disulfide systems (1 - H4CysS2+, 2 - H2Cyst2+, 3 - H4HCysS2+, 4 - H2DTDPA) at 0.25 M HCl
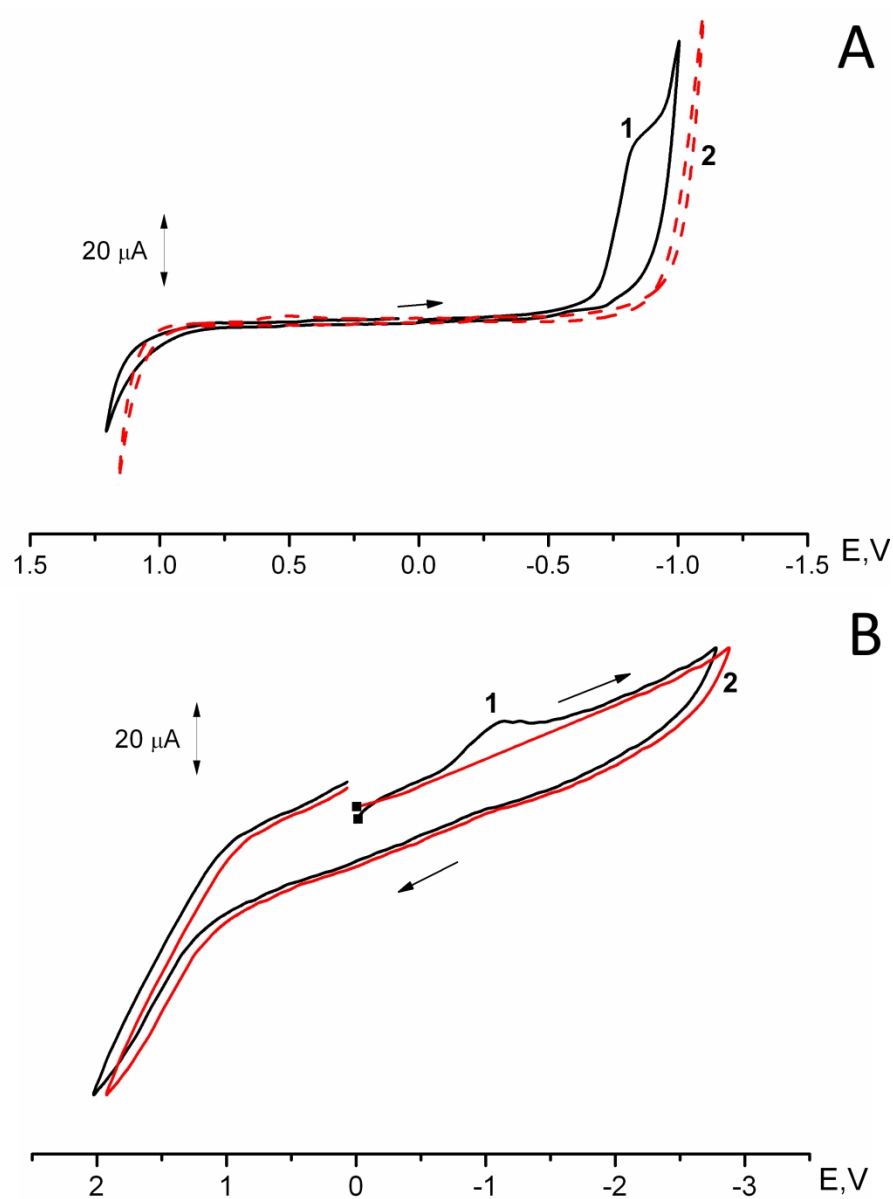
277x198mm (300 x 300 DPI)

1
2
3
4
5
6
7
8
9
10
11
12
13
14
15
16
17
18
19
20
21
22
23
24
25
26
27
28
29
30
31
32
33
34
35
36
37
38
39
40
41
42
43
44
45
46
47
48
49
50
51
52
53
54
55
56
57
58
59
60



Figure 4. Cyclic voltammograms of Pt(II) - H4CysS2+ system in aqueous hydrochloric solution (G, dэ = 5 mm, 0.25 M HCl, C = 2.5 mM, V vs SCE, scan rate 25 mV s-1 ) and [Pt(SCH2CH2CO2H)2Cl2] complex in DMSO containing 0.1 M TBAHFP (C = 2 mM scan rate 100 mV/s); 1 – complex, 2 – background

226x304mm (300 x 300 DPI)
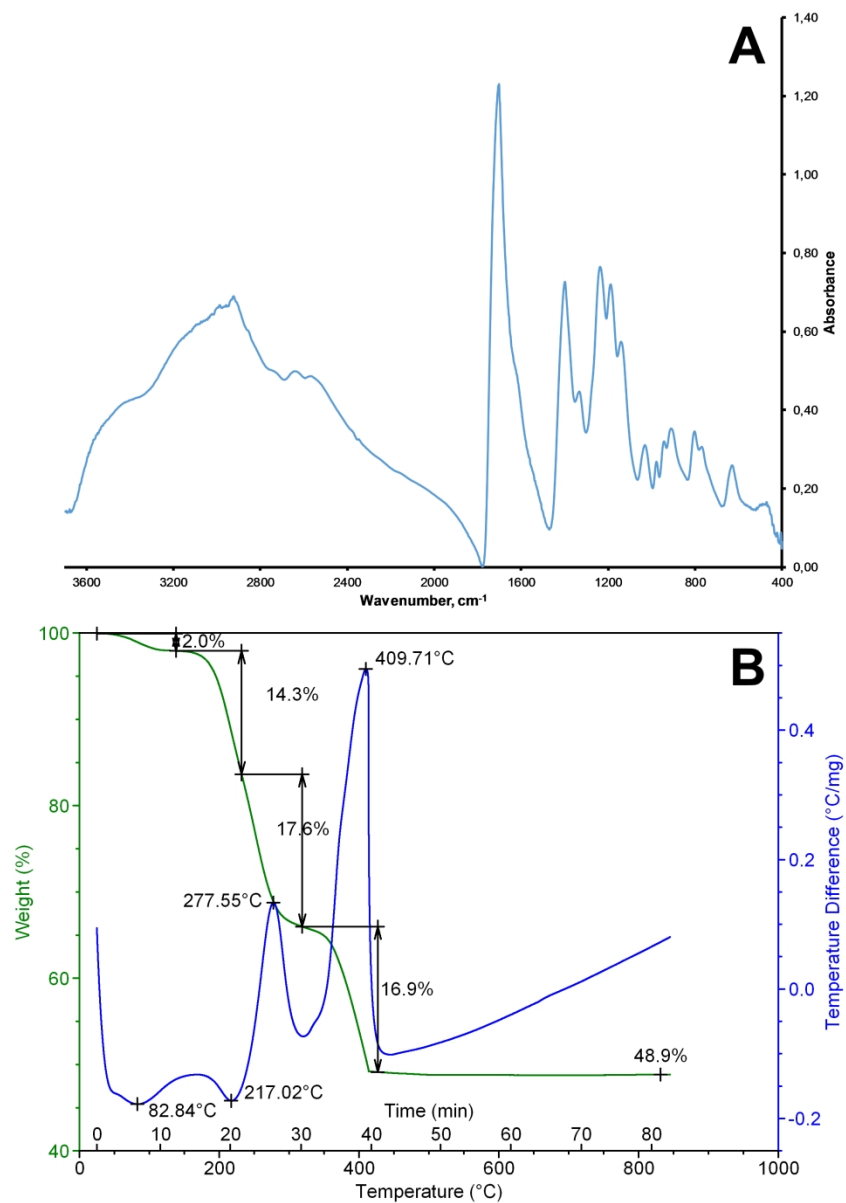
Figure 5. IR spectra (A) and TGA/DSC curves (B) for [Pt(SCH2CH2CO2H)2Cl2] complex

218x296mm (300 x 300 DPI)
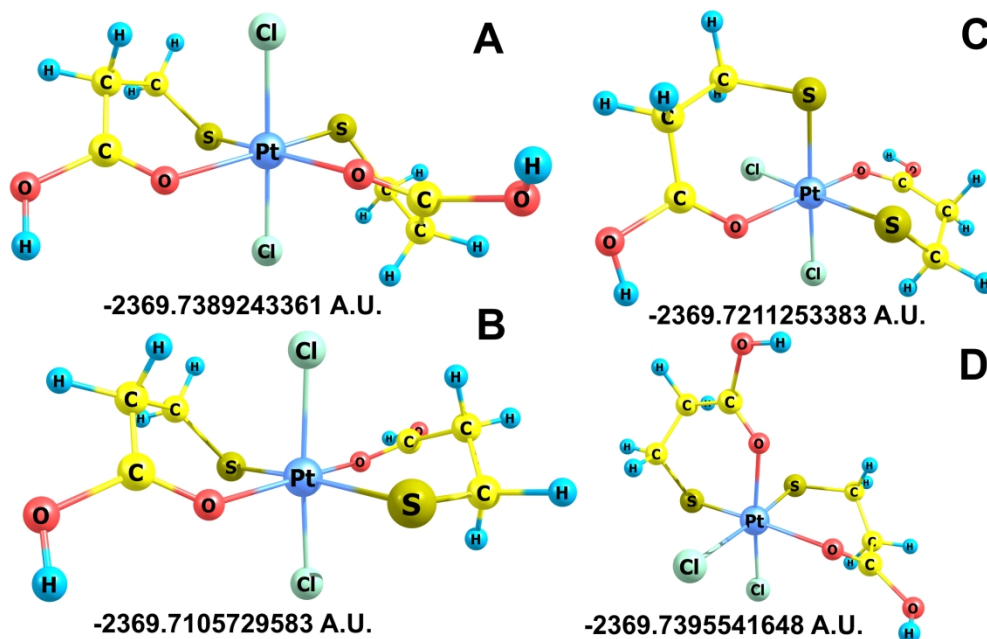
Figure 6. DFT optimized structures of the [Pt(SCH2CH2CO2H)2Cl2] at PBE0-D3/Def2-SVP level

214x135mm (300 x 300 DPI)

Figure 7. Molar ratio method (A) for systems  Au(III) - disulfides (1 - H4CysS2+, 2 - H2DTDPA, 3 - H2Cyst2+, 4 - H4HCysS2+) and  Raman spectra (B) of  Au(III) - H2DTDPA (1) and H2DTDPA - H2O2 (2) systems in 0.25 M HCl

335x118mm (300 x 300 DPI)

Scheme 1. Proposed thermal fragmentation of [Pt(SCH2CH2CO2H)2Cl2] complex

228x42mm (300 x 300 DPI)

1
2
3
4
5
6
7
8
9
10
11
12
13
14
15
16

# Interaction of Pt(II) and Au(III) with organic disulfide in hydrochloric aqueous solution
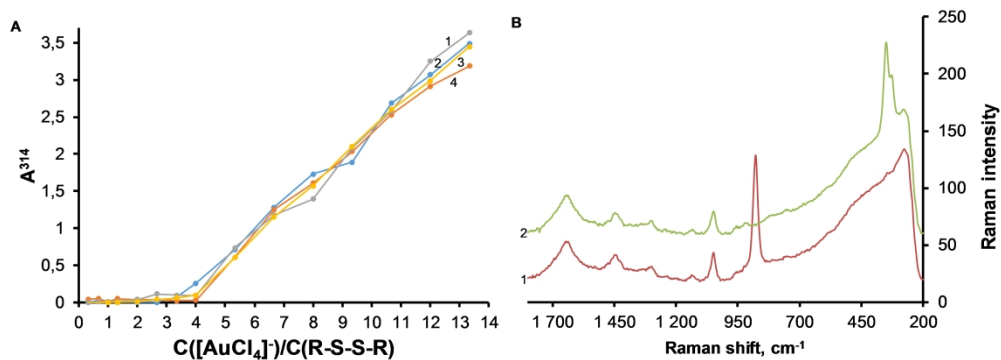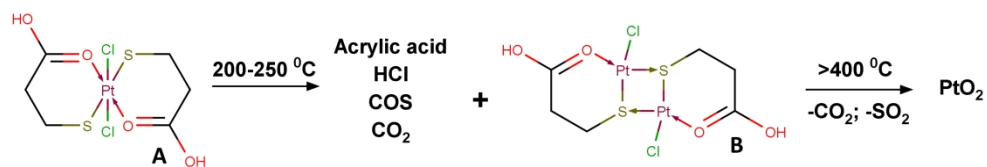
Alexander I. Petrov[*a], Galina V. Novikova[b], Anastasia V. Demina[b], Timur Y. Ivanenko[b], Elizaveta S. Goleva[b],

[a] Institute of Chemistry and Chemical Technology SB RAS, Federal Research Center "Krasnoyarsk Science Center SB RAS", Krasnoyarsk, Russian Federation
[b] Institute of Non-Ferrous Metals and Materials Science, Siberian Federal University, Krasnoyarsk, Russian Federation

*Corresponding author, E-mail: sfupetrov@gmail.com

17
18
19
20
21
22
23
24
25
26
27
28
29
30
31
32
33
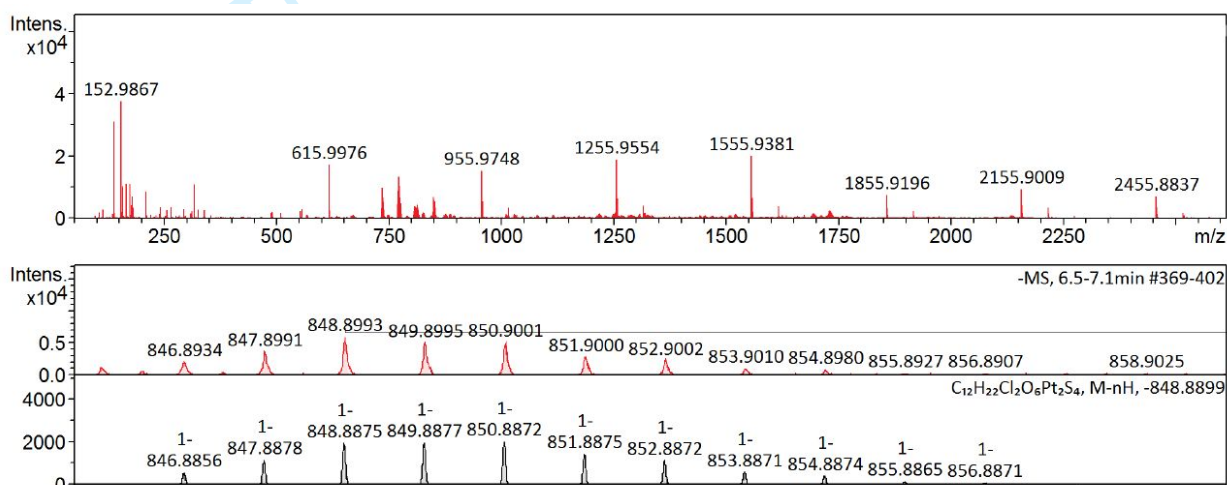


Figure S1. ESI mass spectrum of the complex [Pt(SCH$_2$CH$_2$CO$_2$H)$_2$Cl$_2$] in DMSO obtained in the negative mode (top). ESI-experimental and theoretically calculated isotope patterns of assigned peaks for [Pt$_2$(μ-SCH$_2$CH$_2$CO$_2$H)$_2$Cl$_2$]·2DMSO (bottom)

34
35
36
37
38
39
40
41
42
43
44
45
46
47
48
49
50
51
52
53
54
55
56
57
58
59
60
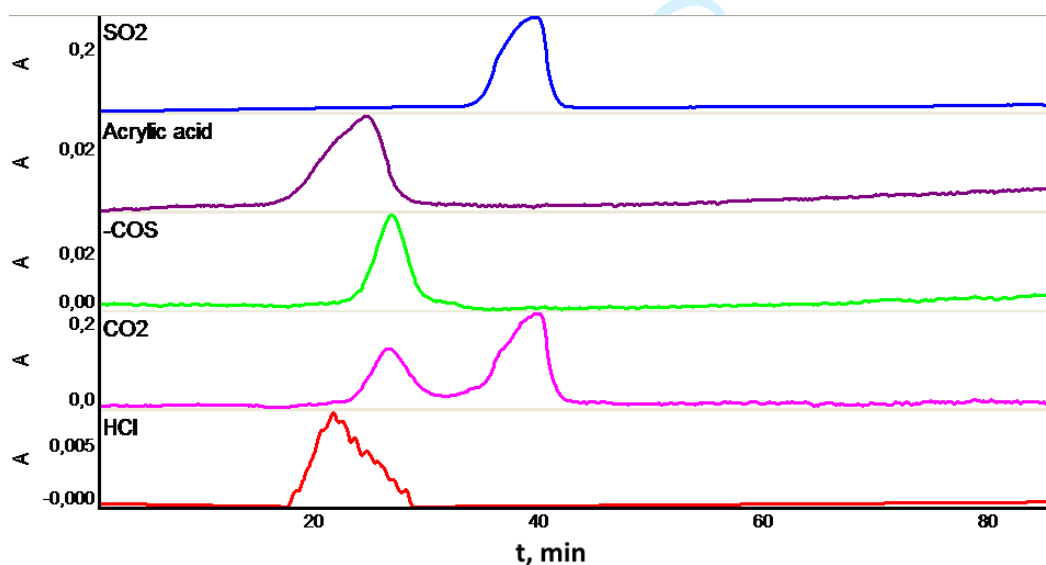


Figure S2. Decomposition products from time to time according to TG-FTIR

1

1
2
3
4
5
6
7
8
9
10
11
12
13
14
15
16
17
18
19
20
21
22
23
24
25
26
27
28
29
30
31
32
33
34
35
36
37
38
39
40
41
42
43
44
45
46
47
48
49
50
51
52
53
54
55
56
57
58
59
60

Optimized Geometries at the at the DEF2-SVP/PBE0-D3 Level of Theory

Isomer A. TOTAL ENERGY = -2369.7389243361

| | | | |
|---|---|---|---|
| S | 0.198806211 | 0.734860398 | -0.360861418 |
| O | -2.141852581 | 1.977897664 | 1.147656448 |
| O | -3.597863873 | 0.342007623 | 1.315388068 |
| C | -2.731506194 | 1.043874879 | 0.615027543 |
| C | -2.640614959 | 0.656835397 | -0.826708429 |
| C | -1.243155329 | 0.319274811 | -1.378361806 |
| H | -3.345091453 | -0.164923975 | -1.010537469 |
| H | -3.597713897 | 0.695276243 | 2.221393122 |
| H | -1.141265294 | 0.772115604 | -2.373123285 |
| H | -1.139188488 | -0.772994605 | -1.485244702 |
| Pt | -0.262584865 | 2.858463637 | 0.355953569 |
| Cl | -1.305975155 | 3.534322364 | -1.630341228 |
| Cl | 0.655647004 | 2.246009698 | 2.424703380 |
| H | -3.000979850 | 1.554137067 | -1.356912664 |
| S | 1.668635323 | 3.778905073 | -0.459052563 |
| C | 2.426368772 | 4.530999480 | 1.008548759 |
| H | 3.191797581 | 5.182313408 | 0.555494530 |
| H | 2.939959347 | 3.762036771 | 1.600345834 |
| C | 0.163081950 | 5.705149132 | 1.464476073 |
| O | -0.684047235 | 4.903933943 | 1.086321200 |
| O | -0.146071361 | 6.982173360 | 1.549802686 |
| H | -1.063484476 | 7.082452549 | 1.243235449 |
| H | 2.037072645 | 6.286624104 | 2.260466590 |
| C | 1.534338497 | 5.361610910 | 1.949598611 |
| H | 1.337412970 | 4.750603591 | 2.846487545 |

Isomer B. TOTAL ENERGY = -2369.7105729583

| | | | |
|---|---|---|---|
| S | 0.204112641 | 0.260366506 | -0.150857020 |
| O | -1.736080716 | 2.316184491 | 0.874600336 |
| O | -3.604411806 | 1.243012278 | 1.153867865 |
| C | -2.548530007 | 1.488333629 | 0.427563267 |
| C | -2.498798307 | 0.831743533 | -0.903369219 |
| C | -1.238531692 | -0.000535658 | -1.221017445 |
| H | -3.417801574 | 0.244564121 | -1.030054386 |
| H | -3.532277858 | 1.753055556 | 1.980671805 |
| H | -0.978672283 | 0.177397120 | -2.274295297 |
| H | -1.479271275 | -1.068372188 | -1.105407899 |
| Pt | 0.126655318 | 2.642159657 | 0.201540054 |
| Cl | -0.490339961 | 3.089020565 | -2.047789918 |
| Cl | 0.897569643 | 2.263005945 | 2.364593166 |
| H | -2.520257966 | 1.685161078 | -1.602795992 |
| S | -0.139083634 | 4.980994986 | 0.704656498 |
| C | 1.533462481 | 5.583103584 | 0.389030884 |
| H | 2.216759413 | 5.295648822 | 1.206654934 |

2

| | | | |
|---|---|---|---|
| H | 1.466125370 | 6.681947751 | 0.399844921 |
| C | 2.599574523 | 3.760438216 | -0.937876332 |
| O | 2.031219061 | 2.791751380 | -0.413884855 |
| O | 3.760393758 | 3.542780880 | -1.494059361 |
| H | 3.953203752 | 2.589735841 | -1.435995951 |
| H | 2.939622544 | 5.801070940 | -1.291850098 |
| C | 2.109738541 | 5.159076150 | -0.963752509 |
| H | 1.308219467 | 5.190372484 | -1.724566680 |

Isomer C. TOTAL ENERGY =   -2369.7211253383

| | | | |
|---|---|---|---|
| S | -0.194773366 | -0.399050253 | 0.474874057 |
| O | -0.840861771 | -1.179821034 | -2.486397487 |
| O | -2.072289899 | -2.928233450 | -2.833860178 |
| C | -1.572819390 | -2.050562707 | -2.002279112 |
| C | -1.909061620 | -2.320428143 | -0.572825500 |
| C | -1.834283980 | -1.155562260 | 0.399622517 |
| H | -2.900339017 | -2.801499733 | -0.569093178 |
| H | -1.771136902 | -2.699447705 | -3.731253125 |
| H | -2.581307441 | -0.388285423 | 0.148847511 |
| H | -2.045545530 | -1.533683824 | 1.412103819 |
| Pt | -0.087995919 | 0.501813404 | -1.700389620 |
| Cl | -2.327903630 | 1.362625899 | -1.611764764 |
| Cl | 0.109413199 | 1.402412798 | -3.918388760 |
| H | -1.182439773 | -3.101873336 | -0.279593507 |
| S | 2.096508238 | -0.385953869 | -1.700429619 |
| H | 4.015541873 | 0.671301395 | -2.590035072 |
| C | 2.978353012 | 1.008575984 | -2.437735969 |
| H | 2.539138698 | 1.243422939 | -3.418241695 |
| C | 2.999663855 | 2.240716140 | -1.549277215 |
| H | 3.496966010 | 2.004463209 | -0.589512191 |
| H | 3.571738339 | 3.067236110 | -2.000014348 |
| C | 1.686120145 | 2.812158647 | -1.127598620 |
| O | 0.588017487 | 2.256478612 | -1.008841326 |
| O | 1.755576701 | 4.064374640 | -0.755481413 |
| H | 0.870009116 | 4.342916122 | -0.461284981 |

Isomer D. TOTAL ENERGY =   -2369.7395541648

| | | | |
|---|---|---|---|
| S | -0.573652542 | 0.533502666 | 0.103046987 |
| O | -2.063978284 | 2.340372817 | -2.256093102 |
| O | -4.260091765 | 2.448480779 | -2.225887912 |
| C | -3.119860859 | 2.058759028 | -1.700282651 |
| C | -3.245333711 | 1.306789657 | -0.418106820 |
| C | -2.049128207 | 1.518022899 | 0.502418665 |
| H | -4.192558389 | 1.604059654 | 0.057200745 |
| H | -4.060585109 | 2.860978121 | -3.084065828 |
| H | -1.802275336 | 2.591306329 | 0.564998972 |
| H | -2.325939895 | 1.193094294 | 1.517550988 |
| Pt | -0.256735620 | 1.074669829 | -2.156085902 |

3

| Cl | -1.552580699 | -0.676094211 | -2.814044597 |
| Cl | 0.203424751 | 1.749649505 | -4.396345778 |
| H | -3.332017812 | 0.239030039 | -0.691876765 |
| S | 1.561929284 | -0.322598274 | -2.101562334 |
| H | 3.797603760 | 0.301121064 | -2.367870083 |
| C | 2.872836928 | 0.898974566 | -2.324177959 |
| H | 2.743326540 | 1.393570060 | -3.299984384 |
| C | 2.999344375 | 1.909176340 | -1.193459944 |
| H | 2.926363514 | 1.392353854 | -0.218448274 |
| H | 3.967136116 | 2.432892826 | -1.214131840 |
| C | 1.932776025 | 2.951909346 | -1.174511308 |
| O | 0.763991332 | 2.818096702 | -1.526261580 |
| O | 2.325064554 | 4.116039808 | -0.709879839 |
| H | 1.559607684 | 4.715267852 | -0.710189496 |

4